A novel immunoregulatory role for NK-cell cytotoxicity in protection from HLH-like immunopathology in mice.

Fernando E Sepulveda, Sophia Maschalidi, Christian A. J. Vosshenrich, Alexandrine Garrigue, Mathieu Kurowska, Gaël Ménasche, Alain Fischer, James P Di Santo, Geneviève de Saint Basile

A novel immunoregulatory role for NK cell cytotoxicity in protection from HLH-like immunopathology in mice

Fernando E. Sepulveda[1,2], Sophia Maschalidi[1,2], Christian A.J. Vosshenrich[3,4], Alexandrine Garrigue[1,2], Mathieu Kurowska[1,2], Gael Ménasche[1,2], Alain Fischer[1,2,5,6], James P. Di Santo[3,4] and Geneviève de Saint Basile[1,2,7].

[1] INSERM UMR1163, Laboratory of Normal and Pathological Homeostasis of the Immune System, F-75015 Paris France.

[2] Paris Descartes University-Sorbonne Paris Cité, Imagine Institute, F-75015 Paris France.

[3] Institut Pasteur, Unité d'Immunité Innée, Département d'Immunologie, Paris, France

[4] Institut Pasteur, INSERM U668, Paris, France

[5] Immunology and Pediatric Hematology Department, Necker Children's Hospital, AP-HP, Paris, France

[6] Collège de France, F-75005 Paris, France

[7] Centre d'Etudes des Déficits Immunitaires, Assistance Publique-Hôpitaux de Paris, Hôpital Necker, Paris, France

Running Title: NK cytotoxicity controls HLH

Key words: HLH, cytotoxic activity, NK cells, CTL

Corresponding authors:

Fernando E. Sepulveda
Inserm U1163, Imagine Institute
Hôpital Necker-Enfants Malades
F-75015 Paris, France
Phone: + 33 142 754 410
Fax: + 33 142 754 225
fernando.sepulveda@inserm.fr

Geneviève de Saint Basile,
Inserm U1163, Imagine Institute
Hôpital Necker-Enfants Malades
F-75015 Paris, France
Phone: +33 142 754 407
Fax: +33 142 754 225
genevieve.de-saint-basile@inserm.fr

Abstract word counts: 171 words
Text word counts: words 4222, figures 6, supplementary figures 3 and references 33.
Regular article: Immunobiology

Key Points

- NK cytotoxic activity limits HLH-like immunopathology in cytotoxic-deficient mice.
- NK cytotoxic activity reduces T cell activation and tissue infiltration of macrophages.

ABSTRACT

The impairment of cytotoxic activity of lymphocytes disturbs immune surveillance and leads to the development of Hemophagocytic lymphohistiocytic syndrome (HLH). Although CTL control of HLH development is well documented, the role for NK cell effector functions in the pathogenesis of this immune disorder remains unclear. In this study, we specifically targeted a defect in cytotoxicity to either CTL or NK cells in mice in order to dissect the contribution of these lymphocyte subsets to HLH-like disease severity after LCMV infection. We found that NK cell cytotoxicity was sufficient to protect mice from the fatal outcome that characterizes HLH-like disease and to reduce HLH-like manifestations. Mechanistically, NK cell cytotoxicity reduced tissue infiltration by inflammatory macrophages and down-modulated LCMV-specific T cell responses by limiting hyper-activation of CTL. Interestingly, the critical protective effect of NK cells on HLH was independent of IFN-γ secretion and changes in viral load. Therefore, our findings identify a crucial role of NK cell cytotoxicity in limiting HLH-like immunopathology, highlighting the important role of NK cytotoxic activity in immune homeostasis.

INTRODUCTION

Cytotoxic T lymphocytes (CTL) and Natural killer (NK) cells play a central role in the defence against viruses and tumours[1]. CTL and NK cells perform their cytolytic function by specifically recognizing and eliminating infected and transformed cells in a process dependent on the polarized secretion of perforin and granzymes at the immunological synapse[1,2]. In humans, the importance of this effector function is highlighted by an immunopathological condition observed in patients with inborn errors affecting lymphocyte cytotoxic function[2,3]. These disorders result in a life-threatening condition known as Hemophagocytic lymphohistiocytic syndrome (HLH), an immune dysregulation characterized by the loss of lymphocytes homeostasis and a severe hyperinflammation[3,4]. HLH patients present with non-remitting fever, hepatosplenomegaly, hypercytokinemia, accumulation of activated CD8 T cells and organ infiltration by activated macrophages that phagocytose cellular elements and red-blood cells (i.e. hemophagocytosis)[4]. In humans, the onset of HLH is believed to be triggered mainly by viral infection, but HLH can also occur in the absence of any detectable pathogen[3,5].

Familial forms of HLH (FHL) are caused by mutations affecting the cytolytic effector protein perforin, or proteins involved in the molecular machinery required for the biogenesis and/or transport of perforin-containing vesicles to the immune synapse[2]. Thus, mutations in perforin (*PRF1*) are responsible for FHL type 2 (FHL2)[6], *UNC13-D* for FHL3[7], *STX11* for FHL4[8] and *STXBP2* for FHL5[9]. HLH can also be presented with hypopigmentation as in Gricelli syndrome type 2 (*RAB27A*) and Chediak-Higashi syndrome (*LYST*)[10-12].

Our understanding of the immunopathological mechanisms responsible for HLH development has benefited from the availability of several murine models of HLH. Cytotoxic-deficient mice (such as *Prf1*, *Rab27a*, *Unc13d*, *Stx11* and *Lyst* mice) develop a severe HLH-like syndrome after infection with lymphocytic choriomeningitis virus (LCMV)[13-18]. In the absence

of cytotoxic activity of CD8 T cells, an accumulation of the antigen-presenting cells that continuously activate CTL was reported in *Prf1*-/- mice[19]. The hyper-activated CTL secrete high levels of IFN-γ, which appears critical for the development of HLH-like symptoms[13,20]. MyD88 signalling is also thought to be important for HLH-like development, since in *Unc13d Myd88* double knock-out mice a reduction in CTL and macrophage activation has been observed[21]. The crucial role of CTL and IFN-γ for HLH-like development has been highlighted by experiments where depletion of CTL or blocking of IFN-γ, prevents and reduces HLH-like manifestations, respectively[13,17,20]. Despite the fact that injection of anti-NK1.1 depleting antibodies in *Prf1*-/- mice did not prevent development of HLH-like symptoms[13], the contribution of NK cytotoxic activity to HLH immunopathogenesis has not been fully addressed. Recently, NK cells were shown to play an important immunoregulatory role by limiting hyper-activation of CTL in a mechanism dependent on perforin[22-24]. Whether or not a similar mechanism may participate in the pathogenesis of HLH is unknown.

In this study, we dissect the specific contribution of NK cell cytotoxic activity to HLH development. By generating murine models in which cytotoxic defects are restricted to CTL or NK cells, we show that both CTL and cytotoxic NK cells contribute to the development of HLH-like syndrome in mice after LCMV infection. Interestingly, our results show that the mechanism by which the cytotoxic function of CTL and NK cells prevents HLH-like manifestations differs. Whereas CTL cytotoxicity mainly acts on viral clearance, NK cytotoxic activity limits hyper-activation of CTL and tissue infiltration by activated macrophages. Thus, our data show that these cytotoxic lymphocytes subsets play non-redundant roles in immune homeostasis and the prevention of LCMV-induced immunopathology.

METHODS

Mice. *Stx11*$^{flox/flox}$, *Stx11*-/-, C57BL/6J wt and C57BL/6J-*Prf1*^{tm1Sdz}/J have been described previously[16]. *Ncr1*^{greenCre} mice were described previously[25]. C57BL/6J *Rag2*-/- *Il2rg*-/- CD45.2 and C57BL/6J *Rag2*-/- CD45.1 mice were kindly provided by Dr. Benedita Rocha (INEM, Paris). P14 CD45.1 mice were described previously[16]. P14 *Prf1*-/- CD45.1 mice were generated by breeding P14 CD45.1 mice with *Prf1*-/- CD45.2 mice. Mice were maintained in pathogen-free conditions and handled according to national and institutional guidelines.

Induction of HLH-like syndrome by LCMV infection. The WE strain of LCMV was kindly provided by Professors Maries van de Broek and Rolf Zinkernagel (University of Zürich, Switzerland). Mice aged 8-14 weeks received an i.p. injection of 200 pfu. Blood counts were checked after infection using an automated cell counter (the MS 9-5 V, Melet Schloesing Laboratories). Serum levels of alanine and aspartate aminotransferase were determined using the VetTest® Chemistry Analyzer (IDEXX Laboratories). The serum IFN-γ concentration was determined using an ELISA kit (eBioscience). The serum levels of other cytokines and chemokine were quantified by CBA kit (BD Bioscience).

LCMV viral load was assessed by quantitative PCR as described previously[16]. Briefly, cDNA was isolated from tissue samples and analyzed with primers for LCMV (forward: 5'-TCTCATCCCAACCATTTGCA-3' and reverse: 5'-GGGAAATTTGACAGCACAACAA-3') and β-actin (forward: 5'-CCAGCAGATGTGGATCAGCA-3' and reverse: 5'-CTTGCGGTGCACGATGG-3') using SYBR Green PCR Master Mix (Applied Biosystems).

***In vitro* CD8$^+$ T and NK cell activation and degranulation assays.** Spleen CD8$^+$ T cells were purified from the spleen and activated *in vitro* with a T cell activation/expansion kit (Miltenyi) in the presence of 50 U/ml of recombinant IL-2. After 5 days, T cell degranulation

was assayed by activating 4 x 10^5 cells with different concentrations of anti-CD3e (clone 500A2, eBioscience) in the presence of PE-coupled anti-CD107a (clone 1D4B, eBioscience) antibody. Degranulation capacity was assayed in $CD8^+$ T cells and compared with non-activated cells and the corresponding isotype control.

NK cells were purified from the spleen by negative selection (Miltenyi, NK isolation kit) and cultured *in vitro* in the presence of 50 ng/ml IL-15 for 7 days. NK degranulation was assessed following incubation with YAC-1 target cells.

***In vivo* T cell proliferation.** To measure T cell proliferation, 1 x 10^6 CFSE-labeled perforin-sufficient or -deficient P14 CD45.1 CD8 T cells were transferred i.v. into mice carrying perforin-sufficient or perforin-deficient T cells mice, respectively at day -1. At day 0, recipient mice were infected with 200 pfu of LCMV i.v. Three days later, CFSE dilution was assessed by FACS analysis (gated on $CD8^+$ $CD45.1^+$ cells).

NK cell depletion. Starting at day -2, anti-NK1.1 depleting antibody (clone PK136) was administrated by i.p. injection (50 ug) every 3 days in order to deplete NK1.1 expressing cells. Under these conditions, more than 90% of NK deletion in blood was achieved (data not shown). At day 0 mice were infected with a single dose of 200 p.f.u. of LCMV and HLH-like syndrome was evaluated as previously described[16].

Bone-marrow reconstitution. For bone marrow transfer, 3 weeks old *Rag2*-/- *Il2rg*-/- CD45.2 and *Rag2*-/- CD45.1 mice were injected i.v. with 2 x 10^7 marrow cells from control or *Prf1*-/- mice. Immune reconstitution was monitored by FACS analysis and by measuring total lymphocytes blood counts using an automated cell counter (the MS 9-5 V, Melet Schloesing Laboratories). After at least 8 weeks of marrow transfer and complete immune reconstitution,

mice were challenged with 200 p.f.u of LCMV to induce HLH-like syndrome as described above.

Statistical analysis. Data were analyzed with GraphPad Prism 6 software. Survival curves were analyzed using the log-rank test. All other analyses were performed using *t*-tests or one-way ANOVA with posttest. Differences were considered to be statistically significant when $p < 0.05$ (indicated as *$p<0.05$, **$p<0.01$ and ***$p<0.001$).

RESULTS

Natural killer cell cytotoxic activity reduces HLH-like manifestations in mice

It has been extensively documented that cytotoxicity-deficient CD8 T cells are the main driving force for immunopathogenesis in mouse models of HLH-like disease[13,17,19,26]. In contrast, the contribution of NK cells to HLH-like manifestations is less clear. Depletion of NK cells in *Prf1*-/- mice did not prevent HLH-like development, suggesting that NK cells were dispensable for the initiation of this syndrome[13]. To specifically determine the contribution of NK cells in the development of HLH-like disease, we utilized LCMV-infected perforin-deficient mice, as these mice develop a disease pathology that closely mimics human HLH. We generated chimeric mice by transferring bone marrow from control or *Prf1*-/- mice on the CD45.2 background into *Rag2*-/- *Il2rg*-/- CD45.2 (lacking both, T and NK populations) or *Rag2*-/- CD45.1 (lacking only T cells) mice. Following BM transfer, primary and secondary lymphoid organs were repopulated with mature T and NK cells (Supplementary Figure 1A). When *Rag2*-/- *Il2rg*-/- mice were reconstituted with control or *Prf1*-/- BM as donor cells, both T and NK cells were CD45.2, i.e., cytotoxic proficient ($T^{Prf1+}NK^{Prf1+}$ mice) or deficient ($T^{Prf1-}NK^{Prf1-}$ mice) respectively. In contrast, when *Rag2*-/- CD45.1 mice were reconstituted with *Prf1*-/- BM, T cells were cytotoxic deficient since they developed from donor cells (CD45.2), whereas NK cells were cytotoxic proficient since they were endogenously (CD45.1) derived ($T^{Prf1-}NK^{Prf1+}$ mice) (Supplementary Figure 1B).

To determine the contribution of NK cytotoxic activity to HLH-like development, we infected $T^{Prf1+}NK^{Prf1+}$, $T^{Prf1-}NK^{Prf1-}$ and $T^{Prf1-}NK^{Prf1+}$ mice with a single dose of 200 p.f.u. of LCMV. As expected, upon LCMV injection, $T^{Prf1+}NK^{Prf1+}$ mice survived the infection, whereas mice in which both T and NK cells were deficient in cytotoxic activity, succumbed before 28 days post-infection (Figure 1A). Besides the increased susceptibility to LCMV, $T^{Prf1-}NK^{Prf1-}$ mice presented a significant loss of body weight and a dramatic drop in body temperature

compared with $T^{Prf1+}NK^{Prf1+}$ mice (Figure 1A). Interestingly, the presence of cytotoxic NK cells in an otherwise perforin-deficient recipient ($T^{Prf1-}NK^{Prf1+}$ mice) could significantly prolong survival after infection (Figure 1A). $T^{Prf1-}NK^{Prf1+}$ mice presented with an intermediate phenotype in terms of body weight and body temperature. Compared to control mice, $T^{Prf1-}NK^{Prf1-}$ mice presented the typical biological features of HLH-like immunopathology, including leukopenia, decreased numbers of red-blood cells, haematocrit and platelets and lack of neutrophilia on day 14 post-infection (Figure 1B-1D). In contrast, $T^{Prf1-}NK^{Prf1+}$ mice displayed normal RBC and platelet counts on day 14 post-infection (Figure 1C), although blood leukocyte numbers were reduced compared to $T^{Prf1+}NK^{Prf1+}$ mice (Figure 1B, 1D).

An HLH-like syndrome in $T^{Prf1-}NK^{Prf1-}$ mice was associated with splenomegaly and liver-infiltration by activated immune cells (Figure 2A, 2B). Interestingly, splenomegaly and liver-infiltration after LCMV infection was comparable between $T^{Prf1+}NK^{Prf1+}$ and $T^{Prf1-}NK^{Prf1+}$ mice (Figure 2A, 2B). MNC liver-infiltrate in $T^{Prf1-}NK^{Prf1-}$ mice was highly enriched in activated CD8 T cells, while percentage and absolute numbers of these cells were lower in $T^{Prf1+}NK^{Prf1+}$ and $T^{Prf1-}NK^{Prf1+}$ mice (Figure 2C). Strikingly, similar absolute numbers of liver-infiltrating NK cells were detected in all three conditions, indicating that phenotypic differences between $T^{Prf1-}NK^{Prf1-}$ and $T^{Prf1-}NK^{Prf1+}$ mice were qualitative (Figure 2C). Tissue-infiltration of macrophages is one of the hallmarks of HLH, and macrophages are one of the most important effector populations in the later phases of HLH immunopathology. Interestingly, macrophage liver-infiltration on day 14 post-infection was significantly reduced in $T^{Prf1+}NK^{Prf1+}$ and $T^{Prf1-}NK^{Prf1+}$ mice, as compared to fully cytotoxic-deficient mice (Figure 2D). Reduction of inflammatory macrophages (defined as $CD64^{+}$ $Ly6C^{+}$ cells[27,28]) infiltration in $T^{Prf1-}NK^{Prf1+}$ mice was observed both in terms of percentage and absolute numbers compared to $T^{Prf1-}NK^{Prf1-}$ mice (Figure 2D). Interestingly, reduced numbers of inflammatory macrophages correlated

with a reduction in levels of serum liver transaminases (ALAT and ASAT) in $T^{Prf1+}NK^{Prf1+}$ and $T^{Prf1-}NK^{Prf1+}$ mice compared to mice that lacked all cytotoxic activity (Figure 2E).

IFN-γ is known to be a critical factor in LCMV-induced HLH-like syndrome, since *in vivo* neutralization of IFN-γ can reduce HLH-like manifestations in mice[13,20]. To determine whether or not the moderate HLH-like manifestations observed in $T^{Prf1-}NK^{Prf1+}$ mice correlated with reduced levels of IFN-γ secretion, we measured IFN-γ production on day 8 post-infection. As expected, $T^{Prf1-}NK^{Prf1-}$ mice had higher levels of IFN-γ compared to $T^{Prf1+}NK^{Prf1+}$ mice (Figure 2F). Interestingly, $T^{Prf1-}NK^{Prf1+}$ mice displayed similar serum IFN-γ levels as $T^{Prf1-}NK^{Prf1-}$ mice (Figure 2F) suggesting that reduction of HLH-like manifestations in the presence of cytotoxic proficient NK cells was not mediated by a reduction in serum IFN-γ levels. HLH-like syndrome is characterized by production of high levels of inflammatory cytokines that contribute to the hyper inflammatory environment. Interestingly, serum levels of inflammatory cytokines and chemokines, including IL-6, CCL2, and CCL5, were similar in $T^{Prf1-}NK^{Prf1-}$ and $T^{Prf-}NK^{Prf+}$ mice (Figure 2G).

Overall, these data show that when cytotoxic potential in mice is strictly limited to NK cells, HLH-like disease manifestations triggered by LCMV infection are dramatically reduced compared to mice that globally lack cytotoxic activity.

Reduction of HLH-like manifestations in $T^{-}NK^{+}$ mice is independent of viral load

Defective viral control and persistent LCMV infection are considered key factors in HLH-like pathogenesis. To address whether the reduction of HLH-like manifestations in mice carrying cytotoxic-proficient NK cells was accompanied by a more efficient viral clearance, we measured viral load in the liver 14 and 21 days upon infection in $T^{Prf1+}NK^{Prf1+}$, $T^{Prf1-}NK^{Prf1-}$ and $T^{Prf1-}NK^{Prf1+}$ mice. Cytotoxic proficient $T^{Prf1+}NK^{Prf1+}$ mice were able to control LCMV replication and successfully cleared the virus (Figure 3). In contrast, cytotoxic-deficient T^{Prf1-}

NK^{Prf1-} mice were unable to control the virus and displayed a high LCMV load (Figure 3). Interestingly, $T^{Prf1-}NK^{Prf1+}$ mice were unable to control LCMV replication and showed similar viral titers as compared to mice that were completely deficient in cytotoxicity (Figure 3). Similar results were observed in the spleen 14 days after LCMV infection (Supplemental Figure 2). Thus, these data show that the improvement of HLH-like manifestations associated with cytotoxic-proficient NK cells appears to be independent of viral replication control *in vivo*.

***In vivo* depletion of cytotoxic proficient Natural Killer cells restores HLH-like syndrome severity**

In order to determine whether the improvement of HLH-like manifestations observed in $T^{Prf1-}NK^{Prf1+}$ mice was dependent on NK cells and not on the presence of other innate lymphocyte population present in *Rag2-/-* mice, we compared HLH-like manifestations of LCMV infected $T^{Prf1-}NK^{Prf1+}$ mice after NK cell depletion. Mice were injected with an anti-NK1.1 depleting antibody every third day, starting 2 days before infection. As previously shown, upon infection, all $T^{Prf1-}NK^{Prf1+}$ mice survived whereas $T^{Prf1-}NK^{depleted}$ mice were highly susceptible to LCMV infection (Figure 4A). In parallel, NK depletion in $T^{Prf1-}NK^{Prf1+}$ mice led to major loss of body weight and body temperature (Figure 4A) similarly to the ones observed in fully cytotoxic-deficient mice (Figure 1). Depletion of endogenous NK cells in $T^{Prf1-}NK^{Prf1+}$ mice also had an impact on other HLH-like manifestations. At 14 days post-infection, $T^{Prf1-}NK^{depleted}$ mice presented with leukopenia, anaemia, splenomegaly and organ infiltration by total leukocytes and activated macrophages (Figure 4B-4F), similar to mice where both CTL and NK cells populations were cytotoxic-deficient (Figure 1 and Figure 2). Thus, these data show that the improvement of HLH-like manifestations observed in $T^{Prf1-}NK^{Prf1+}$ mice depend on the

presence of endogenous cytotoxic proficient NK cells. In this setting, NK cytotoxic activity appears to be sufficient to partially prevent HLH-like development in mice.

Natural killer cells cytotoxic defect does not induce HLH-like syndrome in mice but causes leukocytosis

These results suggest that NK cytotoxic activity contributes to prevent HLH-like development by a mechanism independent of viral clearance. In order to determine whether defective NK cytotoxic activity was sufficient to induce HLH-like development upon viral infection, we studied a second mouse model in which a defect in cytotoxicity was restricted to NK cells. As mice harbouring a conditional perforin allele are not yet available, we created mice with a NK cell-specific ablation of Stx11, a protein that is required for release of perforin-containing cytotoxic granules[16,17,29]. We crossed *lox*P-flanked *Stx11* mice[16] with a transgenic mouse line expressing Cre recombinase under the promoter of NKp46 (Ncr1)[25] that allows for specific ablation of Stx11 expression in NK cells ($T^{+}NK^{Stx11-}$ mice). As control, we used littermate Ncr1cre-*Stx11*+/+ mice. $T^{+}NK^{Stx11-}$ mice developed normally, were fertile and showed no variations in the percentage of lymphoid and myeloid cell populations compared to littermate controls (data not shown). As expected, NK cells from $T^{+}NK^{Stx11-}$ mice failed to degranulate *in vitro*, whereas CD8 T cells degranulated normally upon CD3/CD28 activation as assessed by CD107 expression (Supplemental Figure 3).

In order to determine whether defective NK cell cytotoxic activity was sufficient to induce HLH-like development, control, *Stx11*-/- and $T^{+}NK^{Stx11-}$ mice were injected with a single dose of LCMV (200 p.f.u.). While control mice restrain LCMV infection successfully, Stx11-deficient mice developed most clinical and biological features of HLH-like syndrome including loss of body weight (Figure 5A), drop in body temperature (Figure 5A), hunched posture, lethargy, pancytopenia (Figure 5B and C) and lack of neutrophilia (Figure 5D). In

contrast to complete Stx11-deficient mice, $T^{+}NK^{Stx11-}$ mice did not develop HLH-like manifestations and were similar to control mice in terms of body weight, temperature, RBC and platelet counts and hematocrit (Figures 5A,C).

Whereas complete Stx11-deficient mice developed a severe leukopenia and neutropenia upon LCMV infection, $T^{+}NK^{Stx11-}$ mice presented a significant leukocytosis, even compared to control mice (Figure 5B and 5D). $T^{+}NK^{Stx11-}$ mice had higher numbers of neutrophils and CD4 and CD8 lymphocytes in the blood at 12 days post infection (Figure 5D-F and data not shown). $T^{+}NK^{Stx11-}$ mice presented intermediate levels of serum IFN-γ compared to control and complete Stx11-deficient mice (Figure 5G). Interestingly, in accordance with the lack of HLH-like manifestations, $T^{+}NK^{Stx11-}$ mice completely eliminated the virus 21 days after infection, suggesting that CD8 T cell cytotoxic activity was sufficient to control LCMV (Figure 5H).

These data show that the restricted defect of cytotoxic activity in NK cells was not sufficient to induce HLH-like immunopathology in mice, as far as $T^{+}NK^{Stx11-}$ mice were able to control LCMV infection. Nonetheless, the absence of cytotoxic function in NK cells correlated with an exacerbated leukocytosis and a limited secretion of IFN-γ, suggesting a regulatory role for NK cells in lymphocytes proliferation and in mounting a physiologic response against LCMV infection.

Natural killer cells cytotoxic activity controls T cell response *in vivo*.

Taken together, the beneficial role of natural killer cell cytotoxic activity in alleviating HLH-like manifestations as observed in $T^{Prf1-}NK^{Prf1+}$ mice (Figure 1) and the differential immune response observed in LCMV-infected $T^{+}NK^{Stx11-}$ mice (Figure 5) suggest that NK cytotoxic activity modulates CTL proliferation upon LCMV viral infection. To test this hypothesis, we assessed CD8 T cell proliferation in $T^{Prf1-}NK^{Prf1+}$ and $T^{+}NK^{Stx11-}$ mice and compared them with

their respective controls. We adoptively transferred perforin-sufficient or -deficient CFSE labelled P14 TCR transgenic CD8 T cells into $T^{Prf1+}NK^{Prf1+}$, $T^{Prf1-}NK^{Prf1-}$ and $T^{Prf1-}NK^{Prf1+}$ mice which were subsequently infected with 200 p.f.u. LCMV. Three days after infection, CFSE dilution was analyzed as a measure of CTL proliferation. Although LCMV titers were similar in all conditions (data not shown), P14 CD8 T cells had a higher proliferative capacity in $T^{Prf1-}NK^{Prf1-}$ mice as compared to $T^{Prf1+}NK^{Prf1+}$ mice (Figure 6A). In $T^{Prf1-}NK^{Prf1+}$ mice, P14 CD8 proliferation was similar to the level observed in $T^{Prf1+}NK^{Prf1+}$ mice (Figure 6A). Accordingly, absolute numbers of P14 CD8 cells were significantly higher in the spleen of complete cytotoxic-deficient mice compared with control $T^{Prf1+}NK^{Prf1+}$ mice (Figure 6B). Strikingly, the presence of NK cytotoxic proficient cells reduced absolute numbers of P14 CD8 T cells in the spleen to values similar to those seen in $T^{Prf1+}NK^{Prf1+}$ mice (Figure 6B). Interestingly, during the course of the anti-LCMV response, activation of endogenous CD8 T cells was also reduced in $T^{Prf1-}NK^{Prf1+}$ mice compared with fully cytotoxic-deficient mice. The fraction of $KLRG1^+$ $Ly6C^+$ among endogenous CD8 T cells was 2-fold increased in $T^{Prf1-}NK^{Prf1-}$ mice compared to $T^{Prf1+}NK^{Prf1+}$ and $T^{Prf1-}NK^{Prf1+}$ mice (Figure 6C).

To determine the impact of defective NK cytotoxic activity on CTL activation, we adoptively transferred perforin-sufficient or -deficient P14 cells to control, *Stx11*-/- and T^+NK^{Stx11-} mice and 3 days after LCMV infection, P14 cell proliferation was assessed. P14 cell proliferation was found significantly higher in fully cytotoxic deficient mice compared to control mice in terms of P14 cells, presenting a higher percentage of cells in proliferation and total number of P14 cells present in the spleen (Figure 6D). Notably, in T^+NK^{Stx11-} mice P14 CD8 T cells proliferated significantly more compared to control mice, as a higher percentage of P14 cells presented increased number of division cycles (Figure 6D). The absolute counts of P14 cells per spleen were moderately increased in T^+NK^{Stx11-} mice as compared to those measured in the spleen of control mice (Figure 6E). Altogether, these results show that NK cell cytotoxic

activity controls activation of cytotoxic CD8 T cells, suggesting that in a cytotoxic deficient host, the loss of such a mechanism could contribute to the hyper activation of lymphocytes in the settings of LCMV infection, which is a hallmark of the immunopathological events responsible for HLH-like development.

DISCUSSION

In the current study, we dissected the specific roles for cytotoxic NK and T cells to HLH-like development, by targeting the cytotoxic defect to each of the two main cytotoxic lymphocyte populations. Firstly, we found that in mice, CD8 T cells with impaired cytotoxicity (perforin-deficient CTL) are not sufficient to induce the full clinical picture of HLH-like syndrome. HLH-like syndrome with all clinical signs only develops when also NK cells show defective cytotoxicity. In the case where T cells but not NK cells displayed impaired cytotoxic activity, LCMV-infected mice developed reduced immunopathology and milder clinical manifestations of HLH-like syndrome, and, more importantly survived LCMV challenge that was lethal for mice harbouring non-cytotoxic lymphocytes. Secondly, we demonstrated that defective NK cytotoxic activity was not sufficient to induce HLH-like syndrome but was nevertheless associated with transient lymphocytosis. During the acute phase of the antiviral response against LCMV infection, we observed an exacerbated and transient expansion of lymphocytes, culminating to a robust immune response and a successful viral clearance in conditional NK-cytotoxic deficient mice. Other reports have shown similar results in models of acute LCMV viral infection, where depletion or absence of NK cells favours a stronger CD8 T cell response and more efficient viral clearance[22,23]. Altogether, our study emphasizes the critical immunoregulatory role of NK cell cytotoxicity during anti-viral immune response and HLH-like development, adding thus a new layer of complexity regarding the contribution of perforin-dependent mechanisms to the regulation of immune homeostasis.

Natural killer cells control the immune response by secreting cytokines, controlling antigen presentation and directly killing infected or tumour transformed cells[30]. There is growing evidence that NK cells control CD8 T cells response via a perforin-dependent mechanism by limiting CD4 help during early stages of CTL activation and differentiation and/or by direct killing of early-activated CTL[22,23]. Several NK receptors have been shown to participate in

this process, especially NKG2D and NKp46[23,31]. Recently, it has been shown that during early stages of anti LMCV response, CTL can escape NK surveillance by increasing the expression of MHC-I inhibitory NK ligands and by decreasing the expression of activating NK receptor ligands in a type I IFN dependent process[31,32]. In our study, by using either bone marrow reconstituted or conditional knock-out mice we show that i) the presence of NK cytotoxic proficient cells restrains accumulation of LCMV specific CD8 T cells and ii) that, defective NK cell cytotoxicity correlates with a higher proliferation rate of antigen-specific CTL. Whether NK cells modulate CD8 T cell responses by direct or indirect NK-T cell recognition and the specific receptors involved in this process is a matter of further investigations.

Our study demonstrates that NK cell cytotoxic activity is essential for preventing HLH-like development caused by LCMV infection in mice. We speculate that by doing so, NK cells can directly limit CTL hyper activation and/or function. Another possibility is that NK cells also interfere with the effector phase of HLH-like syndrome by targeting activated macrophages and limiting therefore tissue destruction. Importantly, the diminished immunopathology observed in $T^{Prf1-}NK^{Prf1+}$ mice supports both hypotheses as far as it correlated with a reduction in CTL activation and with decreased inflammatory macrophage infiltration in the tissues of infected mice. Notably, our data confirmed previous observation regarding the role of NK cytotoxicity in reducing CTL activation in a disease-relevant context.

Interestingly, the reduction in HLH-like manifestations observed in the presence of NK cytotoxic activity was independent of IFN-γ levels and viral load after infection. The persistent viral infection observed in mice carrying cytotoxic proficient NK cells underlines the prominent role of CD8 T cells in LCMV clearance. Indeed, defective NK cytotoxic activity did not prevent normal LCMV clearance. This emphasises the concept that in cytotoxic-deficient mice, viral infection is required to trigger HLH-like syndrome but does not correlate with the course of the disease.

We and others have shown the principal role of IFN-γ in HLH-like development caused by LCMV[13,20]. Strikingly, the beneficial effect of NK cytotoxic activity in reducing HLH-like pathology was not related to a decrease in IFN-γ serum levels in $T^{Prf1-}NK^{Prf1+}$ mice, as it would have been expected. However, IFN-γ levels were measured in the serum and this does not necessarily reflect the actual concentration in the tissue. The cellular source of IFN-γ in the tissues during HLH-like remains a question to be addressed. Furthermore, the sustained secretion of inflammatory cytokines observed in NK proficient mice, suggests that NK cytotoxicity rather interferes directly with effector cells that could be T cells and/or macrophages.

HLH is a heterogeneous syndrome that can present variations in the manifestations and symptoms observed in the patients[3]. Some of these variations can be attributed to the nature of the genetic cause, environmental factors, etc. Whether some of these variations can be attributed to residual cytotoxic activity in one of the two main lymphocyte populations might be an appealing possibility. The fact that residual NK cytotoxic activity can improve HLH-like manifestations puts forward alternative therapeutic options that include the stimulation of complement-dependent cytotoxic mechanisms to eliminate hyper activated CD8 T cells by the administration of Fc-fusion(s) proteins targeting the receptors/ligands involved in this cytotoxic process, as it has been proposed in an experimental tumour model[33].

In this report we have highlighted a previously unappreciated role of NK cytotoxicity in immune homeostasis by dissecting the specific contribution of NK and CD8 T cells to HLH-like development, suggesting that cytotoxic lymphocytes (both CTL and NK cells) regulate the final outcome of immune response and the balance between physiological and pathological condition by a variety of additive and complex cellular mechanisms beyond viral clearance.

Acknowledgement

The authors thank Corina Dragu and Imagine Institute's animal facility for their assistance. FES was supported by fellowships from the Association pour la Recherche sur le Cancer and Becas Chile. SM was supported by fellowships from the Association pour la Recherche sur le Cancer and the Imagine Foundation. This work was supported by the French National Institute of Health and Medical Research (INSERM), the Agence National de la Recherche (ANR HLH-Cytotox/ANR-12-BSV1-0020-01), the ARC Foundation (grant PJA 2013120047), the European Research Council (ERC; PIDImmun, advanced grant 249816) and the Imagine Foundation.

Authorship

Contribution: F.E.S. designed, conducted and analysed experiments with the assistance of A.G and M.K.; S.M. designed, conducted and analysed experiments; C.V. and J.P.D. generated and provided Ncr1^{greenCre} mice, provided tools and valuable discussion; G.M. and A.F. interpreted and discussed data; F.E.S. and S.M. prepared the manuscript figures; F.E.S., S.M. and G.d.S.B. wrote the manuscript; F.E.S., S.M., A.F., J.P.D and G.d.S.B. edited the manuscript; F.E.S. and G.d.S.B. designed and supervised the overall research.

Conflict-of-interest disclosure: The authors declare no competing financial interests.

REFERENCES

1. Voskoboinik I, Smyth MJ, Trapani JA. Perforin-mediated target-cell death and immune homeostasis. *Nat Rev Immunol*. 2006;6(12):940-952.
2. de Saint Basile G, Menasche G, Fischer A. Molecular mechanisms of biogenesis and exocytosis of cytotoxic granules. *Nat Rev Immunol*. 2010;10(8):568-579.
3. Pachlopnik Schmid J, Cote M, Menager MM, et al. Inherited defects in lymphocyte cytotoxic activity. *Immunol Rev*. 2010;235(1):10-23.
4. Henter JI, Horne A, Arico M, et al. HLH-2004: Diagnostic and therapeutic guidelines for hemophagocytic lymphohistiocytosis. *Pediatr Blood Cancer*. 2007;48(2):124-131.
5. Lipton JM, Westra S, Haverty CE, Roberts D, Harris NL. Case records of the Massachusetts General Hospital. Weekly clinicopathological exercises. Case 28-2004. Newborn twins with thrombocytopenia, coagulation defects, and hepatosplenomegaly. *N Engl J Med*. 2004;351(11):1120-1130.
6. Stepp SE, Dufourcq-Lagelouse R, Le Deist F, et al. Perforin gene defects in familial hemophagocytic lymphohistiocytosis. *Science*. 1999;286(5446):1957-1959.
7. Feldmann J, Callebaut I, Raposo G, et al. Munc13-4 is essential for cytolytic granules fusion and is mutated in a form of familial hemophagocytic lymphohistiocytosis (FHL3). *Cell*. 2003;115(4):461-473.
8. zur Stadt U, Schmidt S, Kasper B, et al. Linkage of familial hemophagocytic lymphohistiocytosis (FHL) type-4 to chromosome 6q24 and identification of mutations in syntaxin 11. *Hum Mol Genet*. 2005;14(6):827-834.
9. Cote M, Menager MM, Burgess A, et al. Munc18-2 deficiency causes familial hemophagocytic lymphohistiocytosis type 5 and impairs cytotoxic granule exocytosis in patient NK cells. *J Clin Invest*. 2009;119(12):3765-3773.
10. Menasche G, Pastural E, Feldmann J, et al. Mutations in RAB27A cause Griscelli syndrome associated with haemophagocytic syndrome. *Nat Genet*. 2000;25(2):173-176.
11. Nagle DL, Karim MA, Woolf EA, et al. Identification and mutation analysis of the complete gene for Chediak-Higashi syndrome. *Nat Genet*. 1996;14(3):307-311.
12. Barbosa MD, Nguyen QA, Tchernev VT, et al. Identification of the homologous beige and Chediak-Higashi syndrome genes. *Nature*. 1996;382(6588):262-265.
13. Jordan MB, Hildeman D, Kappler J, Marrack P. An animal model of hemophagocytic lymphohistiocytosis (HLH): CD8+ T cells and interferon gamma are essential for the disorder. *Blood*. 2004;104(3):735-743.
14. Pachlopnik Schmid J, Ho CH, Diana J, et al. A Griscelli syndrome type 2 murine model of hemophagocytic lymphohistiocytosis (HLH). *Eur J Immunol*. 2008;38(11):3219-3225.
15. Crozat K, Hoebe K, Ugolini S, et al. Jinx, an MCMV susceptibility phenotype caused by disruption of Unc13d: a mouse model of type 3 familial hemophagocytic lymphohistiocytosis. *J Exp Med*. 2007;204(4):853-863.
16. Sepulveda FE, Debeurme F, Menasche G, et al. Distinct severity of HLH in both human and murine mutants with complete loss of cytotoxic effector PRF1, RAB27A, and STX11. *Blood*. 2013;121(4):595-603.
17. Kogl T, Muller J, Jessen B, et al. Hemophagocytic lymphohistiocytosis in syntaxin-11-deficient mice: T-cell exhaustion limits fatal disease. *Blood*. 2013;121(4):604-613.
18. Jessen B, Maul-Pavicic A, Ufheil H, et al. Subtle differences in CTL cytotoxicity determine susceptibility to hemophagocytic lymphohistiocytosis in mice and humans with Chediak-Higashi syndrome. *Blood*. 2011;118(17):4620-4629.
19. Terrell CE, Jordan MB. Perforin deficiency impairs a critical immunoregulatory loop involving murine CD8(+) T cells and dendritic cells. *Blood*. 2013;121(26):5184-5191.

20. Pachlopnik Schmid J, Ho CH, Chretien F, et al. Neutralization of IFNgamma defeats haemophagocytosis in LCMV-infected perforin- and Rab27a-deficient mice. *EMBO Mol Med*. 2009;1(2):112-124.
21. Krebs P, Crozat K, Popkin D, Oldstone MB, Beutler B. Disruption of MyD88 signaling suppresses hemophagocytic lymphohistiocytosis in mice. *Blood*. 2011;117(24):6582-6588.
22. Waggoner SN, Cornberg M, Selin LK, Welsh RM. Natural killer cells act as rheostats modulating antiviral T cells. *Nature*. 2012;481(7381):394-398.
23. Lang PA, Lang KS, Xu HC, et al. Natural killer cell activation enhances immune pathology and promotes chronic infection by limiting CD8+ T-cell immunity. *Proc Natl Acad Sci U S A*. 2012;109(4):1210-1215.
24. Cook KD, Whitmire JK. The depletion of NK cells prevents T cell exhaustion to efficiently control disseminating virus infection. *J Immunol*. 2013;190(2):641-649.
25. Merzoug LB, Marie S, Satoh-Takayama N, et al. Conditional ablation of NKp46 cells using a novel Ncr1 mouse strain: NK cells are essential for protection against pulmonary B16 metastases. *Eur J Immunol*. 2014.
26. Lykens JE, Terrell CE, Zoller EE, Risma K, Jordan MB. Perforin is a critical physiologic regulator of T-cell activation. *Blood*. 2011;118(3):618-626.
27. Gautier EL, Shay T, Miller J, et al. Gene-expression profiles and transcriptional regulatory pathways that underlie the identity and diversity of mouse tissue macrophages. *Nat Immunol*. 2012;13(11):1118-1128.
28. Shi C, Pamer EG. Monocyte recruitment during infection and inflammation. *Nat Rev Immunol*. 2011;11(11):762-774.
29. Bryceson YT, Rudd E, Zheng C, et al. Defective cytotoxic lymphocyte degranulation in syntaxin-11 deficient familial hemophagocytic lymphohistiocytosis 4 (FHL4) patients. *Blood*. 2007;110(6):1906-1915.
30. Long EO, Kim HS, Liu D, Peterson ME, Rajagopalan S. Controlling natural killer cell responses: integration of signals for activation and inhibition. *Annu Rev Immunol*. 2013;31:227-258.
31. Crouse J, Bedenikovic G, Wiesel M, et al. Type I interferons protect T cells against NK cell attack mediated by the activating receptor NCR1. *Immunity*. 2014;40(6):961-973.
32. Xu HC, Grusdat M, Pandyra AA, et al. Type I interferon protects antiviral CD8+ T cells from NK cell cytotoxicity. *Immunity*. 2014;40(6):949-960.
33. Zhang B, Kracker S, Yasuda T, et al. Immune surveillance and therapy of lymphomas driven by Epstein-Barr virus protein LMP1 in a mouse model. *Cell*. 2012;148(4):739-751.

Figure 1. Presence of Natural killer cell cytotoxic activity reduces HLH-like manifestations in mice. *Rag2-/- Il2rg-/-* and *Rag2-/-* mice were reconstituted with BM from *Prf1-/-* and control B6 donors. After 8 weeks, $T^{Prf1-}NK^{Prf1-}$ (open bars/ open squares), $T^{Prf1-}NK^{Prf1+}$ (grey bars/grey circles) and $T^{Prf1+}NK^{Prf1+}$ mice (black bars/black squares) were infected with 200 p.f.u. of LCMV-WE. Clinical and biochemical parameters were determined after infection. (A) Survival, body weight and body temperature. (B) White blood cell counts were analysed on day 14-post infection. (C) Red blood cell, haematocrit and platelets counts on day 14 post-infection. (D) The time course of neutrophils counts. Data (mean ± SEM) are representative of 3-4 independent experiments with at least 3 mice in each group. For survival experiments $T^{Prf1-}NK^{Prf1-}$ (n=10), $T^{Prf1-}NK^{Prf1+}$ (n=9) and $T^{Prf1+}NK^{Prf1+}$ (n=12) mice. Dotted lines represent minimal normal values for control mice. Statistical analysis was performed using log-rank test or one-way ANOVA. **p<0.01. ***p<0.001.

Figure 2. Presence of Natural killer cell cytotoxic activity reduces biological features of HLH-like syndrome. *Rag2-/- Il2rg-/-* and *Rag2-/-* mice were reconstituted with BM from *Prf1-/-* and control B6 donors. After 8 weeks, $T^{Prf1-}NK^{Prf1-}$ (open bars), $T^{Prf1-}NK^{Prf1+}$ (grey bars) and $T^{Prf1+}NK^{Prf1+}$ mice (black bars) were infected with 200 pfu of LCMV-WE. (A) Spleen size expressed as percentage of body weight on day 14-post infection. (B) MNC infiltration in liver on day 14-post infection. (C) Absolute numbers of $CD8^+$ and $NK1.1^+$ in liver. (D) FACS analysis of MNC from liver gated on $CD3^-$ $CD19^-$ $NK1.1^-$ (left panel). Quantification of absolute numbers of $CD64^+$ $Ly6C^+$ in liver on day 14-post infection. (E) Serum alanine and aspartate aminotransferase (ALAT and ASAT respectively) levels in infected mice were analysed on day 14 post-infection. (F) Serum IFN-γ on day 8-post infection. (G) Serum IL-6 (left panel), CCL2 (middle panel) and CCL5 levels (right panel) on day 14 post-infection. Data (mean ± SEM) are representative of 3-4 independent experiments with at least 3 mice in

each group. Dotted lines represent minimal normal values for control mice. Statistical analysis was performed using one-way ANOVA or t test. *p<0.05. **p<0.01.

Figure 3. Defective control of LCMV infection in NK cytotoxic-deficient mice. *Rag2-/- Il2rg-/-* and *Rag2-/-* mice were reconstituted with BM from *Prf1-/-* and control B6 donors. $T^{Prf1-}NK^{Prf1-}$ (open bars), $T^{Prf1-}NK^{Prf1+}$ (grey bars) and $T^{Prf1+}NK^{Prf1+}$ mice (black bars) were infected with 200 p.f.u. of LCMV-WE. 14 days after infection, LCMV titers in the liver were determined. Data (mean ± SEM) are representative of 3 independent experiments. Statistical analysis was performed using t test. **p<0.01.

Figure 4. Improvement in HLH-like manifestations in Prf1-reconstituted Rag2-/- mice depends on NK cells. *Rag2-/-* mice were reconstituted with BM from *Prf1-/-* donors. After 8 weeks, $T^{Prf1-}NK^{Prf1+}$ (black bars/black circles) and $T^{Prf1-}NK^{Prf1+}$ injected with anti-NK1.1 depleting antibody (dashed bars/open circles) were infected with 200 pfu of LCMV-WE. Clinical and biochemical parameters were determined after infection. (A) Survival, body weight and body temperature. (B) White blood cell counts were analysed on day 14-post infection. (C) Red blood cell and haematocrit counts on day 14 post-infection. (D) Spleen size expressed as percentage of body weight on day 14-post infection. (E) MNC infiltration in liver on day 14-post infection. (F) Quantification of absolute numbers of $CD64^+$ $Ly6C^+$ in liver on day 14-post infection. Data (mean ± SEM) are representative of 2 independent experiments with at least 3 mice in each group. Statistical analysis was performed using t test. Dotted lines represent minimal normal values for control mice. *p<0.05. **p<0.01.

Figure 5. Defects of NK cytotoxic activity are not sufficient to induce HLH-like development in mice. *Stx11-/-* (open bars/open squares), T^+NK^{Stx11-} (grey bars/grey circles)

and control (black bars/black squares) mice were infected with 200 p.f.u. of LCMV-WE. Clinical and biochemical parameters were determined after infection. (A) Body weight and body temperature. (B) White blood cell counts were analysed on day 12-post infection. (C) Red blood cell, haematocrit and platelets counts on day 12 post-infection. (D) The time course of neutrophils counts. (E) Lymphocytes counts were analysed on day 12-post infection. (F) Absolute numbers of CD8 lymphocytes in blood on day 12-post infection. (G) Serum IFN-γ on day 8-post infection. (H) LCMV titres in liver on day 21-post infection. Data (mean ± SEM) are representative of 2 independent experiments with at least 3 mice in each group. Dotted lines represent minimal normal values for control mice. Statistical analysis was performed using one-way ANOVA or t test. *p<0.05. ***p<0.001.

Figure 6. NK cytotoxic activity controls T cell activation. (A) *Rag2*-/- *Il2rg*-/- and *Rag2*-/- mice were reconstituted with BM from *Prf1*-/- and control B6 donors. After 8 weeks, reconstituted mice were adoptively transferred with 1 x 10^6 CFSE labelled perforin-sufficient or -deficient P14 cells. The day after, mice were infected with 200 p.f.u. of LCMV-WE. The figure shows representative histograms of CFSE staining in P14 cells 3 days after infection transferred into $T^{Prf1+}NK^{Prf1+}$ (left panel / black bars), $T^{Prf1-}NK^{Prf1-}$ (middle panel / open bars) and $T^{Prf1-}NK^{Prf1+}$ (right panel / grey bars). Graph represents the mean ± SEM values from 2 independent experiments with 3 mice in each group. (B) Absolute numbers of P14 cells per spleen 3 days after infection. Data (mean ± SEM) are representative of 2 independent experiments with 3 mice in each group. (C) $T^{Prf1-}NK^{Prf1-}$ (open bars / middle panel), $T^{Prf1-}NK^{Prf1+}$ (grey bars / right panel) and $T^{Prf1+}NK^{Prf1+}$ mice (black bars / left panel) were infected with 200 pfu of LCMV-WE. The figure shows representative FACS analysis of blood MNC gated on $CD8^+$. Graph represents the quantification of $KLRG1^+$ $Ly6C^+$ $CD8^+$ cells from blood on day 8-post infection. Data (mean ± SEM) are representative of 3-4 independent

experiments. (D) Control (left panel / black bars), *Stx11*-/- (middle panel / open bars) and $T^{+}NK^{Stx11-}$ (right panel / grey bars) mice were adoptively transferred with 1 x 10^6 CFSE labelled perforin-sufficient or -deficient P14 cells. The day after, mice were infected with 200 p.f.u. of LCMV-WE. The figure shows representative histograms of CFSE staining in P14 cells 3 days after infection and the percentages of cells dividing between 0-4 times and more than 4 times. Graph represents the mean ± SEM values from 2 independent experiments with 3 mice in each group. (E) Absolute numbers of P14 cells per spleen 3 days after infection in control (black bars) and $T^{+}NK^{Stx11-}$ (grey bars) mice. Data (mean ± SEM) are representative of 2 independent experiments with 3 mice in each group. Statistical analysis was performed using one-way ANOVA or t-test. *$p<0.05$. **$p<0.01$. ***$p<0.001$.

Figure 1

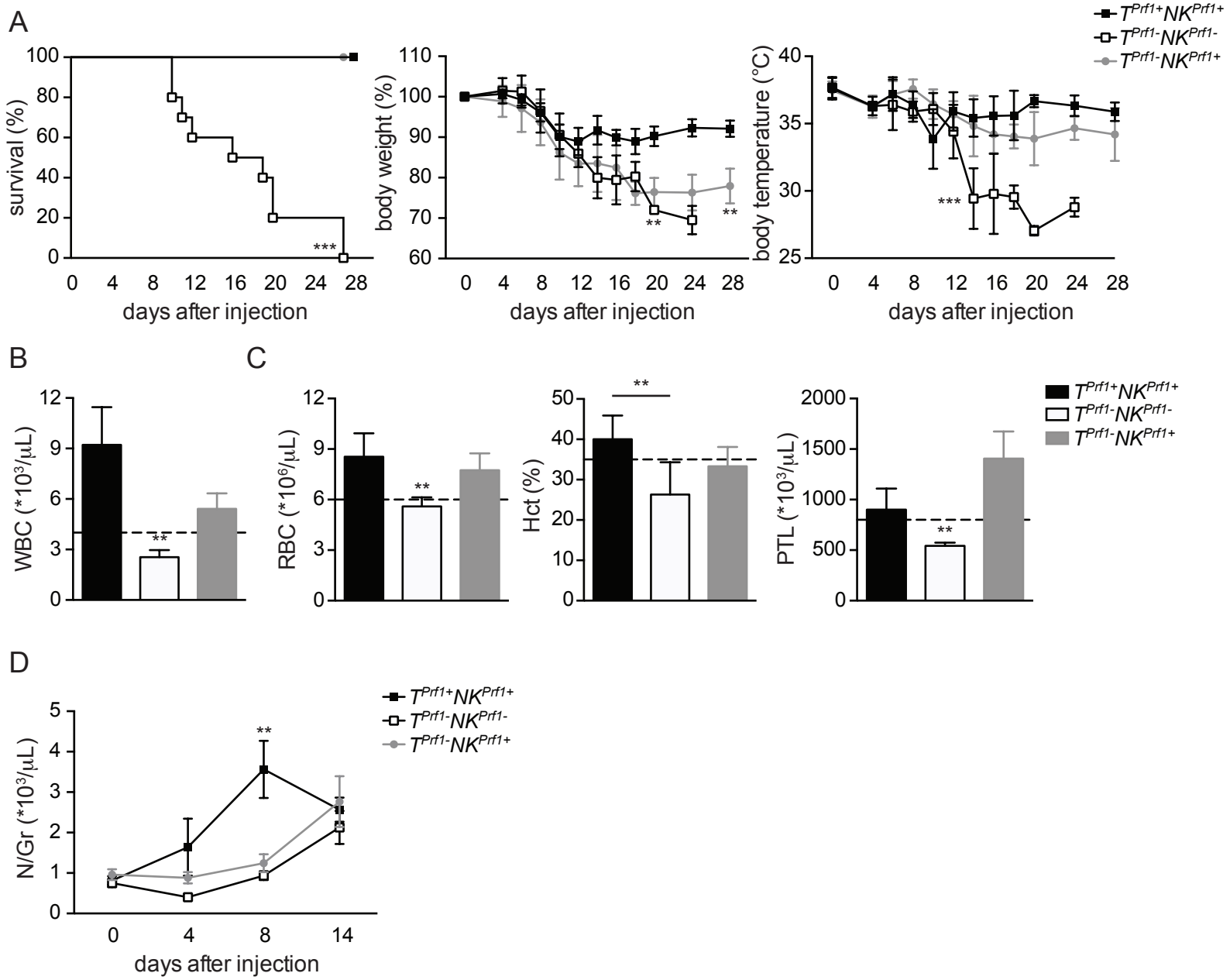
A
$T^{Prf1+}NK^{Prf1+}$
$T^{Prf1-}NK^{Prf1-}$
$T^{Prf1-}NK^{Prf1+}$
survival (%)
days after injection
body weight (%)
days after injection
body temperature (°C)
days after injection
B
WBC (*10³/µL)
C
RBC (*10⁶/µL)
Hct (%)
PTL (*10³/µL)
D
N/Gr (*10³/µL)
days after injection

Figure 2

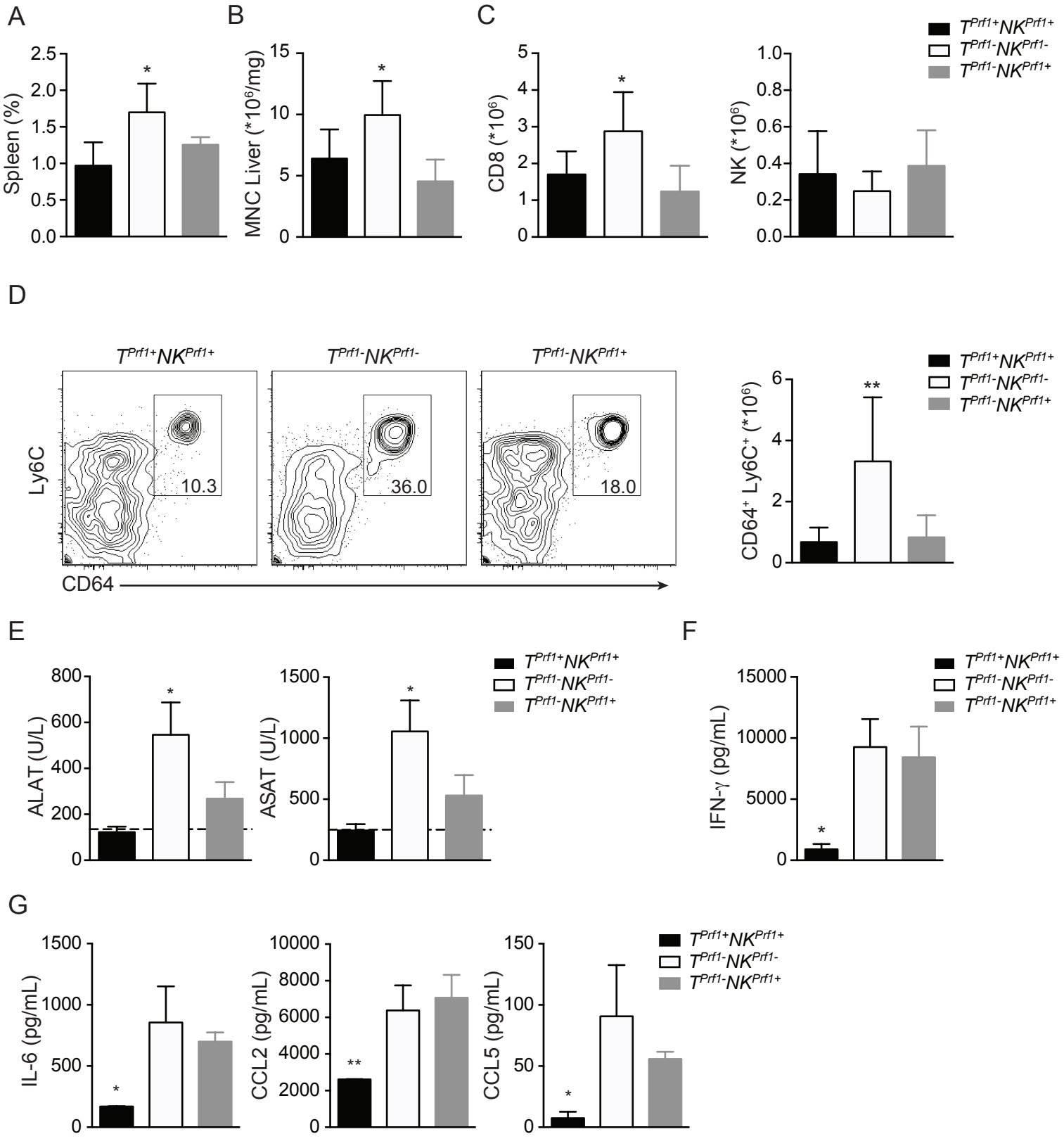
A
B
C
D
E
F
G
Spleen (%)
MNC Liver (*10^6/mg)
CD8 (*10^6)
NK (*10^6)
T^Prf1+NK^Prf1+
T^Prf1-NK^Prf1-
T^Prf1-NK^Prf1+
Ly6C
CD64
10.3
36.0
18.0
CD64+ Ly6C+ (*10^6)
ALAT (U/L)
ASAT (U/L)
IFN-γ (pg/mL)
IL-6 (pg/mL)
CCL2 (pg/mL)
CCL5 (pg/mL)

Figure 3

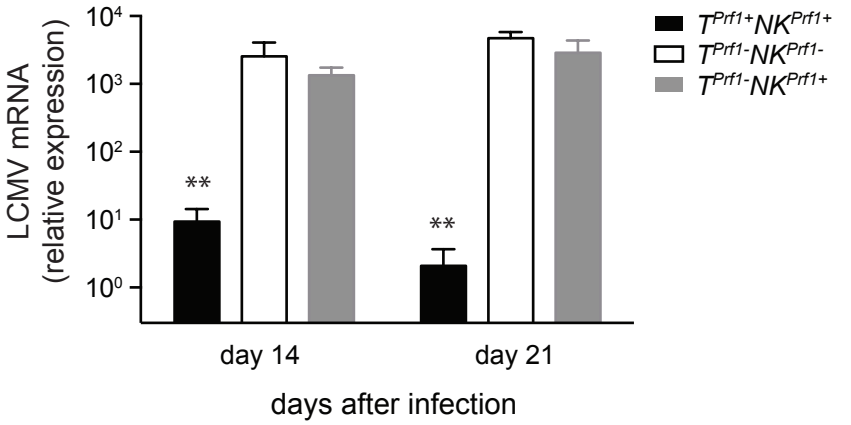
LCMV mRNA
(relative expression)
10^4
10^3
10^2
10^1
10^0
**
**
day 14
day 21
days after infection
$T^{Prf1+}NK^{Prf1+}$
$T^{Prf1-}NK^{Prf1-}$
$T^{Prf1-}NK^{Prf1+}$

Figure 4

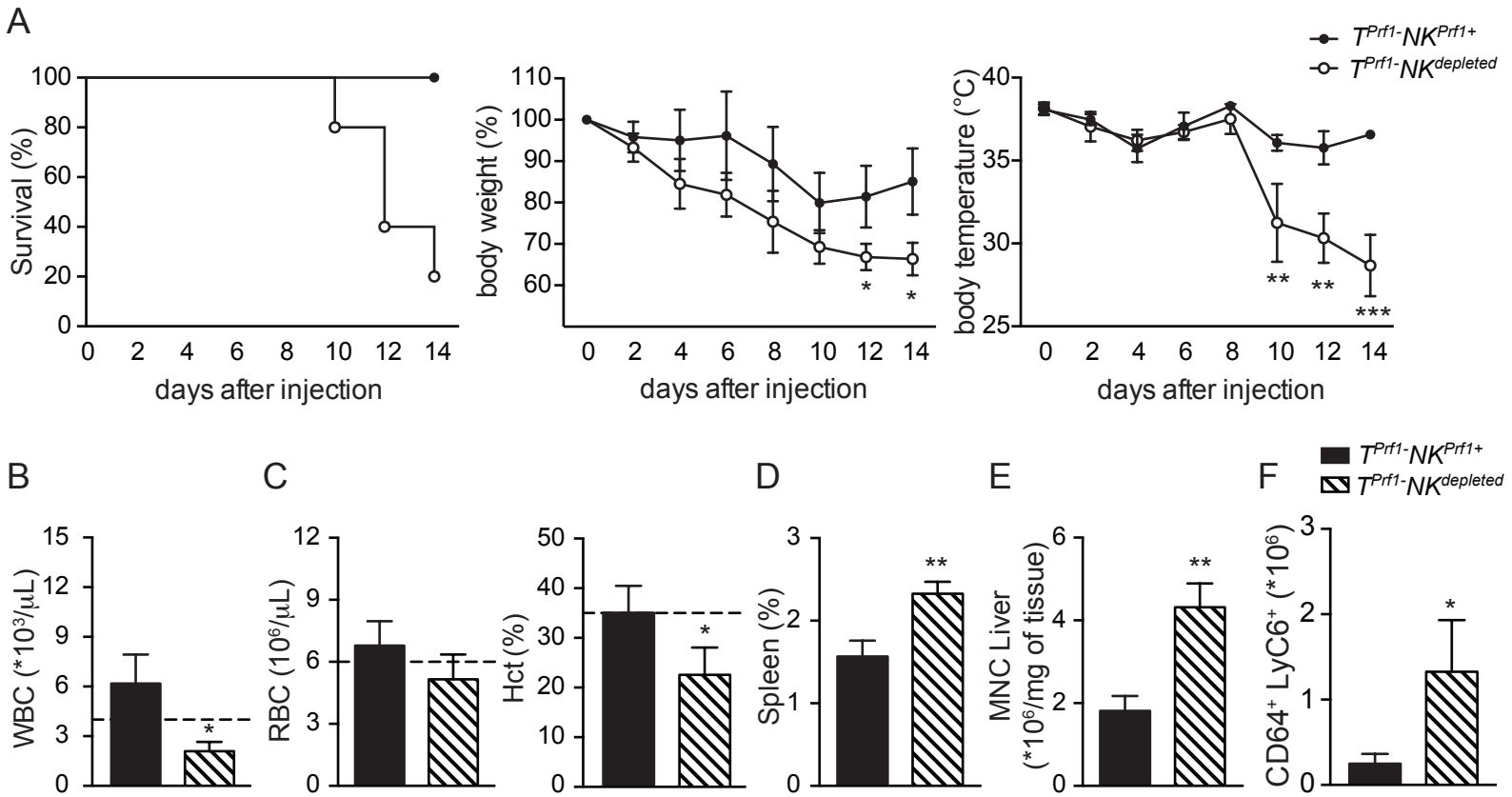
A
Survival (%)
days after injection
body weight (%)
days after injection
body temperature (°C)
days after injection
$T^{Prf1-}NK^{Prf1+}$
$T^{Prf1-}NK^{depleted}$

B
WBC (*10³/µL)
C
RBC (10⁶/µL)
Hct (%)
D
Spleen (%)
E
MNC Liver (*10⁶/mg of tissue)
F
CD64⁺ LyC6⁺ (*10⁶)
$T^{Prf1-}NK^{Prf1+}$
$T^{Prf1-}NK^{depleted}$

Figure 5

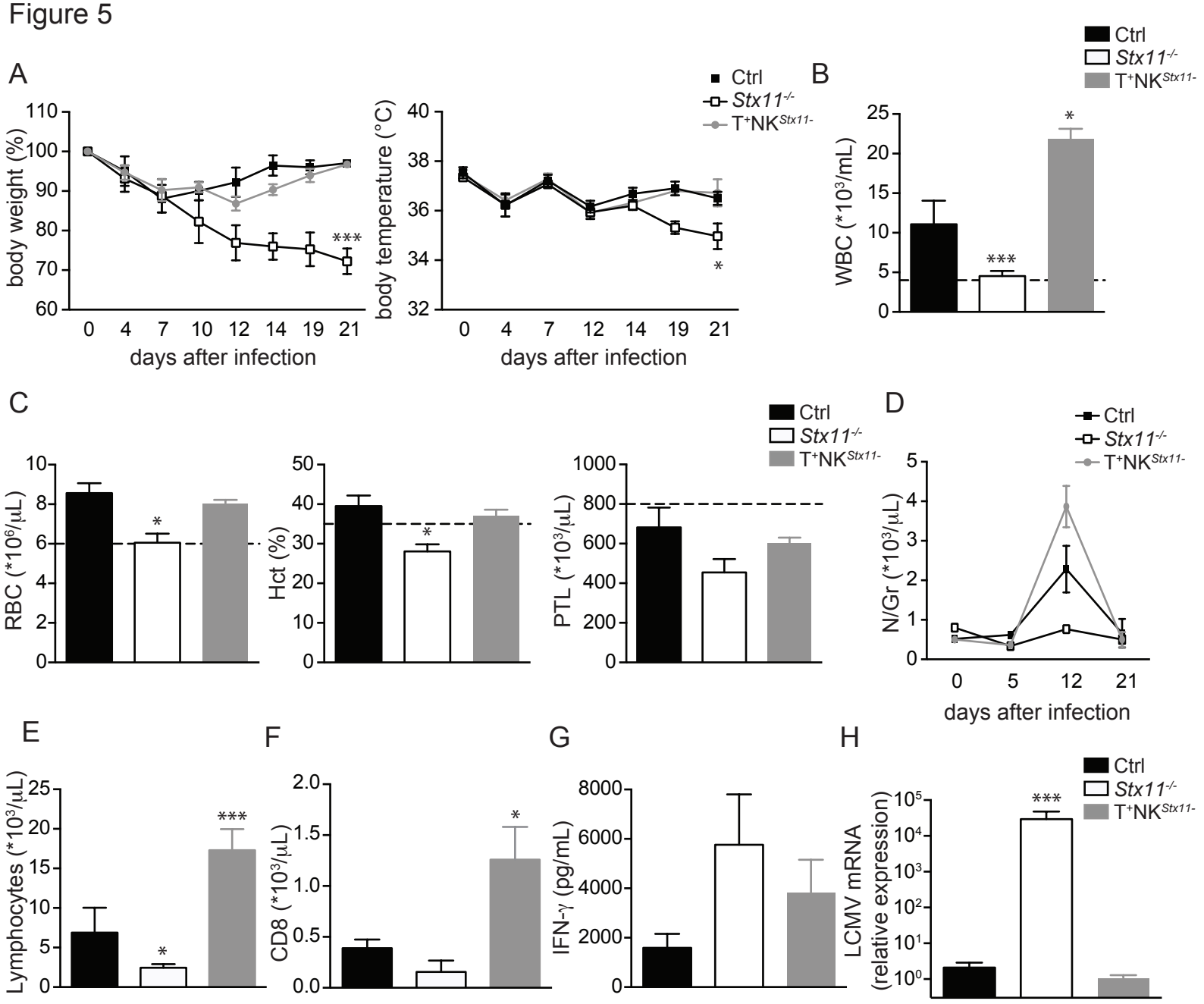
A
body weight (%)
days after infection
body temperature (°C)
days after infection
Ctrl
Stx11-/-
T+NKStx11-
B
WBC (*10³/mL)
C
RBC (*10⁶/µL)
Hct (%)
PTL (*10³/µL)
D
N/Gr (*10³/µL)
days after infection
E
Lymphocytes (*10³/µL)
F
CD8 (*10³/µL)
G
IFN-γ (pg/mL)
H
LCMV mRNA (relative expression)

Figure 6

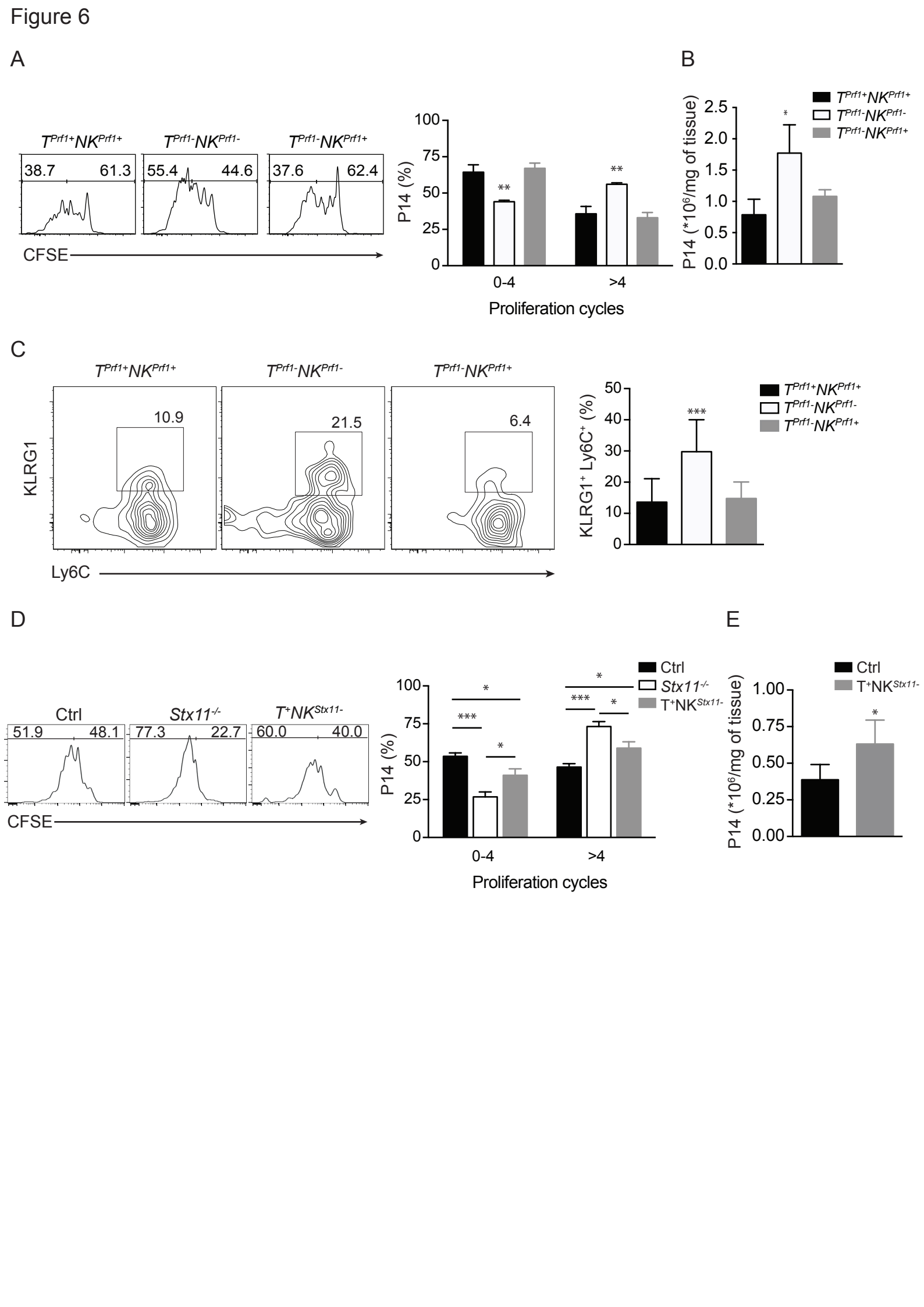
A
B
C
D
E
$T^{Prf1+}NK^{Prf1+}$
$T^{Prf1-}NK^{Prf1-}$
$T^{Prf1-}NK^{Prf1+}$
38.7
61.3
55.4
44.6
37.6
62.4
CFSE
P14 (%)
0-4
>4
Proliferation cycles
P14 (*10⁶/mg of tissue)
KLRG1
Ly6C
10.9
21.5
6.4
KLRG1⁺ Ly6C⁺ (%)
Ctrl
$Stx11^{-/-}$
$T^{+}NK^{Stx11-}$
51.9
48.1
77.3
22.7
60.0
40.0

Supplemental Figure 1. Bone-marrow reconstituted mice. *Rag2-/- Il2rg-/-* and *Rag2-/-* mice were reconstituted with BM from *Prf1-/-* and control B6 donors. (A) White blood cell counts were analysed after 8 weeks of BM transfer on B6 (black squares), *Rag2-/- Il2rg-/-* (open squares), $T^{Prf1-}NK^{Prf1-}$ (open circles), $T^{Prf1-}NK^{Prf1+}$ (grey circles) and $T^{Prf1+}NK^{Prf1+}$ mice (black circles). (B) Representative FACS analysis of CD45.1 and CD45.2 in CD8 T cell (upper row) and NK cell compartment (lower row) measured in the blood of $T^{Prf1+}NK^{Prf1+}$ (left panel), $T^{Prf1-}NK^{Prf1-}$ (middle panel) and $T^{Prf1-}NK^{Prf1+}$ mice (right panel). (C) Graph shows the mean ± SD of $CD45.1^+$ and $CD45.2^+$ NK cells measured in the blood of $T^{Prf1+}NK^{Prf1+}$ (black bars), $T^{Prf1-}NK^{Prf1-}$ (open bars) and $T^{Prf1-}NK^{Prf1+}$ mice (grey bars). Data are representative of 2 independent experiments with n = 4–6 mice per group.

Supplemental Figure 2. Defective control of LCMV infection in NK cytotoxic-deficient mice. *Rag2-/- Il2rg-/-* and *Rag2-/-* mice were reconstituted with BM from *Prf1-/-* and control B6 donors. $T^{Prf1-}NK^{Prf1-}$ (open bars), $T^{Prf1-}NK^{Prf1+}$ (grey bars) and $T^{Prf1+}NK^{Prf1+}$ mice (black bars) were infected with 200 p.f.u. of LCMV-WE. 14 days after infection, LCMV titers in the spleen were determined. Data (mean ± SEM) are representative of 2 independent experiments. ***$p<0.001$.

Supplemental Figure 3. Conditional Stx11-deficient mice present defective NK cell and normal CTL degranulation. (A) Spleen purified NK cells from control (black bar), *Stx11-/-* (white bar) and T^+NK^{Stx11-} mice (grey bar) were expanded in vitro in the presence of recombinant IL-15. Then, degranulation was assessed after activation with YAC-1 cells. Graph shows the mean ± SEM (n =2) of CD107 variation. (B) Spleen CD8 T cells from control, *Stx11-/-* and T^+NK^{Stx11-} mice were activated in vitro. Graphs show the mean ± SEM (n =2) of CD107 variation on CD8 T cells from control (black squares), *Stx11-/-* (open

squares) and $T^{+}NK^{Stx11-}$ (grey circles) mice after stimulation with different concentrations of anti-CD3 antibody.

Supplemental Figure 1

A

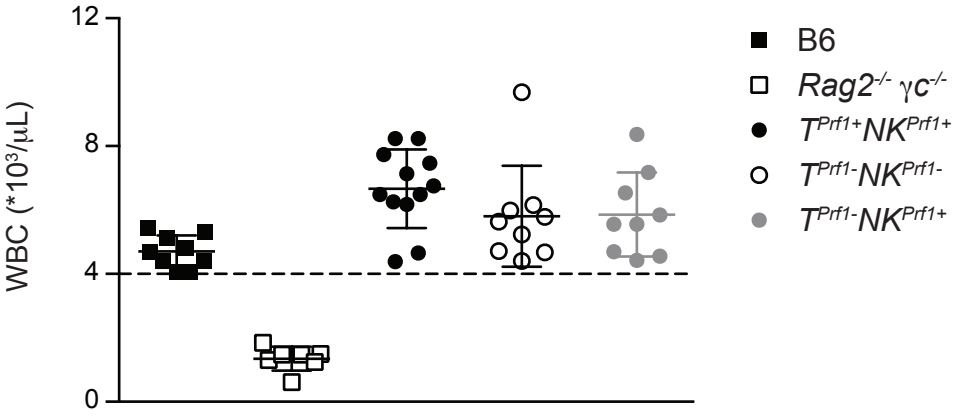

B

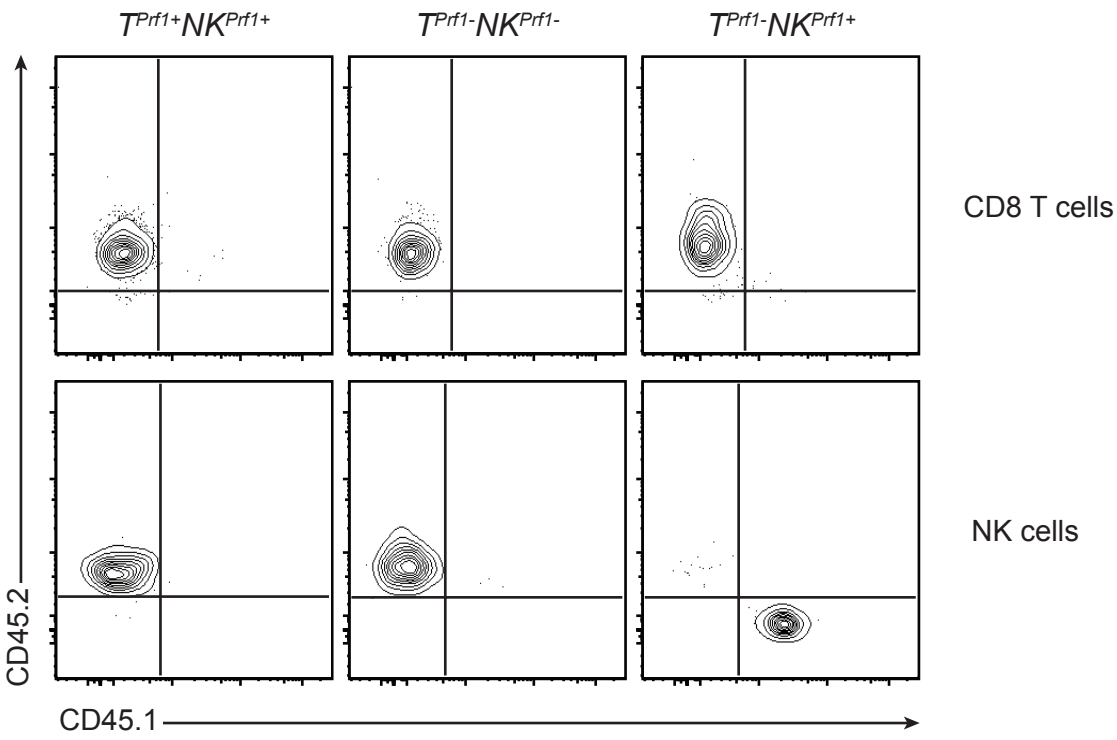

C

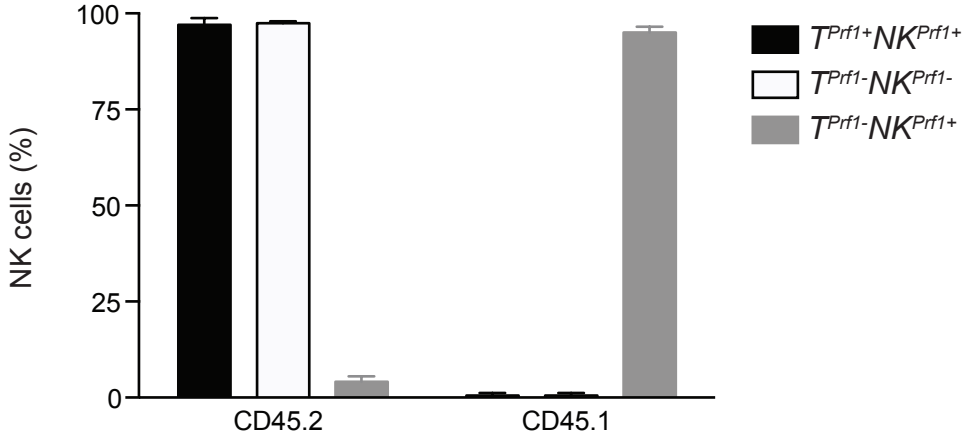

Supplemental Figure 2

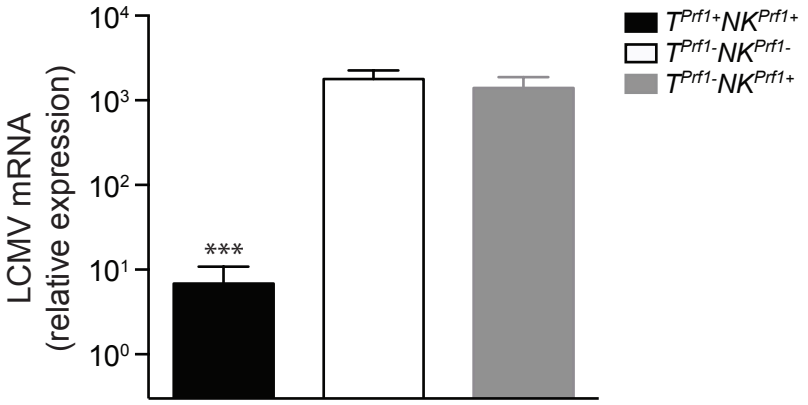

Supplemental Figure 3

A

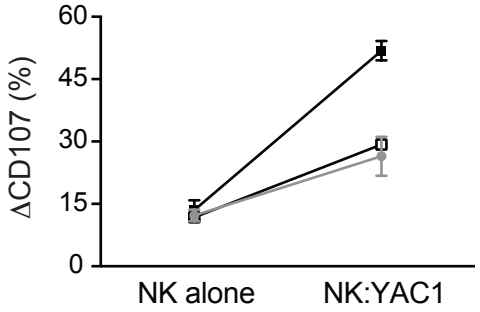

B